Vibrational relaxation of the free terminal hydroxyl stretch in methanol oligomers: Indirect pathway to hydrogen bond breaking

Nancy E. Levinger,[a] Paul H. Davis, and M. D. Fayer
Department of Chemistry, Stanford University, Stanford, California 94305

(Received 12 July 2001; accepted 10 September 2001)

Vibrational relaxation of methanol-*d* (MeOD) in carbon tetrachloride has been investigated via ultrafast infrared pump–probe experiments. Exciting at 2690 cm^{-1}, only the free O-D (where the D is not H-bonded) stretching mode is initially populated. For MeOD mole fractions $\leqslant 0.025$, a 2.15 ps single exponential decay is observed. At mole fractions $\geqslant 0.0375$, the signal decays (2.15 ps decay time) below zero (increased absorption) and then recovers on time scales of 22 ps and $\gg 300$ ps. The increased absorption indicates the formation of additional free ODs caused by the breaking of H-bonds that are not directly coupled to the initially excited vibration. The two-time scale recovery of this signal arises from geminate and nongeminate recombination. The data are fit with a set of kinetic equations that accurately reproduce the data. The results suggest that vibrational relaxation of the initially excited free OD stretch into intramolecular modes of the methanol leads to H-bond breaking. This contrasts studies that suggest direct relaxation of a vibrationally excited OH stretch into an H-bond stretch is responsible for H-bond breaking. © *2001 American Institute of Physics.* [DOI: 10.1063/1.1415447]

I. INTRODUCTION

The ubiquity of hydrogen bonding in chemical and biological systems places it among the most important molecular interactions known. Indeed, many mechanisms in biochemical systems can be attributed to the strong hydrogen bonding found in water.[1–4] While a vast array of experiments have probed hydrogen bonding in a wide range of systems,[5] there remain many questions concerning how hydrogen bonds break and reform in complex media.

Although water is the quintessential hydrogen bond former, other molecules, such as alcohols, display similar hydrogen bond formation. Alcohols are interesting in their own right, and their behavior can provide insights into H-bonding dynamics in water. One advantage of studying alcohols is their solubility in weakly interacting solvents such as carbon tetrachloride (CCl_4) or alkanes. Unlike water, which is only sparingly soluble in nonpolar solvents, alcohols are completely miscible with CCl_4 at all concentrations.[6]

The infrared (IR) spectrum of methanol has been well-studied in solid, liquid, and gas phases. Bertie and Zhang[7,8] have performed an exhaustive study of the methanol IR spectrum, including the various deuterated isotopomers. In the gas phase, the methanol molecules are isolated, but in condensed phases the hydroxyl modes reflect the presence of hydrogen bonding. The steady-state spectrum of methanol in nonpolar solvents has also been studied.[6,9–13] At low concentrations, the spectrum displays only isolated monomeric methanol molecules. Initially, researchers assumed that the sharp feature observed in the OH stretching region reflected only free monomeric methanol molecules.[9,10] Later, others more carefully ascribed the highest energy, spectrally sharp feature to coexisting monomers and terminal OH groups of oligomers that do not donate a hydrogen bond. With increasing concentration, a broad feature appears at lower energies associated with hydrogen bond donating OH groups. At intermediate concentrations, free hydroxyl groups and hydrogen-bonded oligomers appear in the spectrum simultaneously. As the methanol concentration is raised, the molecules form more hydrogen bonds and the spectrum converges to the neat liquid spectrum.

Other groups have probed the dynamics of alcohols in nonpolar solvents.[14–17] Laenen and co-workers[15,16] studied vibrational relaxation of isolated methanol and ethanol in CCl_4 at 0.05 M (~0.5 mol %). At this concentration, virtually all the alcohol molecules present are monomers; thus, they probed dynamics in OH groups that were not hydrogen-bonded. In both systems they observed a transient bleach of the ground vibrational state and a concomitant increased excited-state absorption from the $v=1\rightarrow 2$ transition. They reported vibrational relaxation times, $T_1=9\pm 1$ ps for methanol and $T_1=8\pm 1$ ps for alcohol. Heilweil *et al.*[14] made early measurements on these types of systems but with pulses too long to observe fast transients and with very high powers that may have induced heating artifacts. Analyzing steady-state Raman and IR spectra, Perelygin and Mikhailov[18] reported the vibrational lifetime for nonassociated CH_3OH and CH_3OD in CCl_4 solution to be approximately 1 ps, regardless of deuteration. This result led them to hypothesize that resonant intramolecular energy transfer is not an important pathway for relaxation. The wide range of results reported in the literature indicates that there is no consensus about the dynamics in these systems.

Here, we explore the dynamics following vibrational excitation of the stretching mode of nonhydrogen bond donat-

[a]On sabbatical leave from the Department of Chemistry, Colorado State University, Fort Collins, CO 80523.

ing OD groups in methanol-*d* (CH_3OD, MeOD) dissolved in CCl_4 as a function of the MeOD concentration for a range of concentrations, 1, 2.5, 3.75, and 5 mol %. At all concentrations probed, nonhydrogen-bonded OD groups coexist with hydrogen-bonded groups, although the relative amounts vary. We present data from ultrafast IR pump–probe measurements and a kinetic model to explain the experimental results. For the two lower MeOD concentrations, the data exhibit a 2.15 ps single exponential decay. At the two higher concentrations, the data initially decay with the same 2.15 ps decay time, but the signal also dips below the baseline before recovering. This negative signal recovers at two rates corresponding to 22 ps and $\gg$300 ps recovery times. The negative signal indicates that the absorption of the sample has increased relative to that in the absence of vibrational excitation. The increase in absorption can be caused by H-bond breaking that produces additional MeODs in which the D is not H-bonded. The recovery of the negative signal on the two time scales can arise from geminate and nongeminate recombination. An important point is that H-bonds are broken in spite of the fact that the initially excited vibration resides on an OD in which the D is not H-bonded.

II. EXPERIMENTAL METHODS

Deuterated methanol (Aldrich, 99.5+at. %) and carbon tetrachloride (Aldrich, HPLC grade) were used as received. Samples were prepared by weight at 1, 2.5, 3.75, and 5 mol %. For spectroscopic measurements, home-built copper cuvettes with CaF_2 windows were used. Variable thickness Teflon spacers, 1–2 mm, yielded an absorbance between 0.5 and 1 for all concentrations. In these sample cells the solution came in contact only with the CaF_2 and Teflon, because metals such as copper catalyze the decomposition of MeOD in CCl_4 solution.[19] Steady-state IR spectra measured with an FT-IR (Mattson) were utilized to characterize the samples and revealed no unexpected peaks in the frequency range of the OD stretch.

The laser system used in these experiments consists of a home-built Ti:sapphire oscillator and regenerative amplifier whose output pumps a three-stage optical parametric amplifier (OPA) designed and built in-house to produce tunable midinfrared light (2.5–10 μm or 1,000–4,000 cm^{-1}) of variable pulse duration (150 ps–1.5 ps).[20] The Ti:sapphire oscillator, based on the design of Murnane *et al.*,[21] is pumped by an argon ion laser and runs at 84 MHz, producing $<$50 fs, 4.5 pJ pulses centered at 798 nm.

Before entering the regenerative amplifier, the oscillator pulses are stretched in a single grating/curved mirror stretcher[22,23] of the type first proposed by Martinez.[24,25] In addition, a bandwidth-limiting slit is inserted in a region of the stretcher where the pulse has been spatially separated into its component wavelengths by the grating. By varying the slit width, we select the bandwidth of our laser pulses, and hence the pulse duration. An extracavity Pockels cell placed between the stretcher and the regenerative amplifier selects single pulses at a 1 kHz repetition rate for injection into the amplifier, and home-built electronics synchronize the pulse injection with an intracavity-doubled Q-switched Nd:YLF laser that pumps the amplifier with 11 W of 527 nm light.

The regenerative amplifier employs an in house design.[26,27] The chirped seed from the stretcher is coupled into the cavity through a thin-film polarizer (TFP) and trapped using an intracavity Pockels cell. Two pairs of curved mirrors focus the cavity mode in the Ti:sapphire rod (10 mm long, 0.15% doping, Union Carbide Crystals). After amplification, the pulses are switched out of the cavity by the intracavity Pockels cell. The outgoing amplified pulses are separated from the incoming seed pulses by a Faraday isolator/TFP combination and recompressed in a single grating compressor. The end result is 1.1–1.5$\times$ transform-limited pulses, centered at 798 nm and ranging in pulse duration (depending upon the slit width employed in the stretcher) from $\sim$150 fs to 1.5 ps. The pulse energy is 1.2–1.5 mJ/pulse.

The amplified Ti:sapphire pulses are split into three beams to pump a three-stage optical parametric amplifier (OPA). A white light continuum is generated in sapphire and the resulting near-IR (NIR) radiation is amplified in two OPA stages using Type II BBO. The resultant NIR signal can be tuned between $\sim$1.2 and 1.475 μm (corresponding to an idler wavelength of $\sim$1.74–2.4 μm) by varying the angles of the two BBO crystals. The signal and idler are difference mixed in a Type II $AgGaS_2$ crystal to produce tunable mid-IR (MIR) light in the 1000–4000 cm^{-1} region of the spectrum. For the experiments described here, the Ti:sapphire pump was attenuated prior to the second BBO crystal to avoid saturation of the BBO crystal, and the signal and idler outputs of the second BBO crystal were attenuated to avoid saturation of the $AgGaS_2$ crystal. This resulted in 1–2 μJ MIR pulses centered at 2690 cm^{-1}.

The MIR pulses are split into pump (90%) and probe (10%) beams that traverse different paths before crossing in the sample. The pump beam is chopped at 500 Hz and directed along a variable path length delay line. The probe beam polarization can be rotated by a ZnSe Brewster-plate polarizer in its path. A small amount of the MIR light is split off and used for shot-to-shot normalization. Signal and reference beams impinge on liquid nitrogen cooled MCT detectors whose outputs are processed by gated integrators, divided by an analog processor, and input to a lock-in amplifier. The output of the lock-in is read into a computer using an A/D board.

The IR pulse duration was measured by autocorrelation in a 1 mm Type 1 $AgGaS_2$ crystal. The $<$200 fs pulses were very nearly Gaussian in shape. The spectrum of the pulses was also close to Gaussian. The pulses were always within a factor of 1.15 or less of the transform limit (i.e., 1.15 times the Gaussian time-bandwidth product of 0.44). Extensive tests for power dependence were performed. None of the data changed with the attenuation of either the pump or probe pulses.

III. EXPERIMENTAL RESULTS

Figure 1 displays typical steady-state IR spectra for MeOD in CCl_4 for the concentrations probed, 1, 2.5, 3.75, and 5 mol %. The dramatic change in the MeOD spectrum

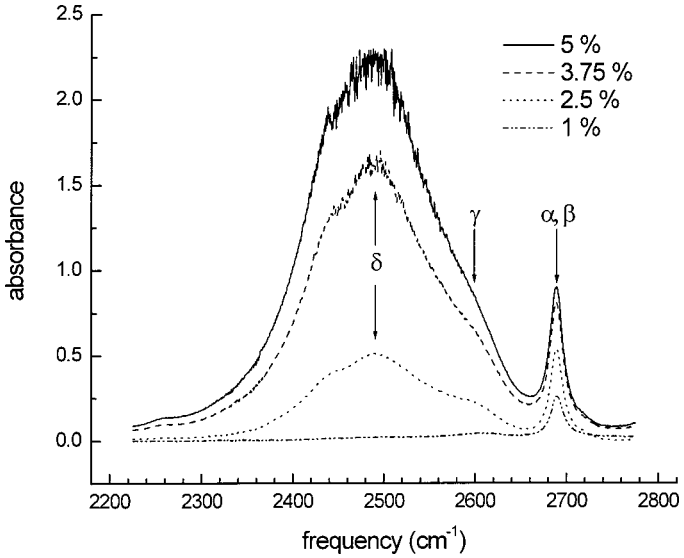

FIG. 1. Steady-state IR spectrum of MeOD in CCl_4 as a function of concentration in mole percent; α refers to isolated monomeric molecules, β to OD oscillators that accept but do not donate hydrogen bonds, γ to molecules donating but not accepting hydrogen bonds, and δ to molecules that both donate and accept hydrogen bonds.

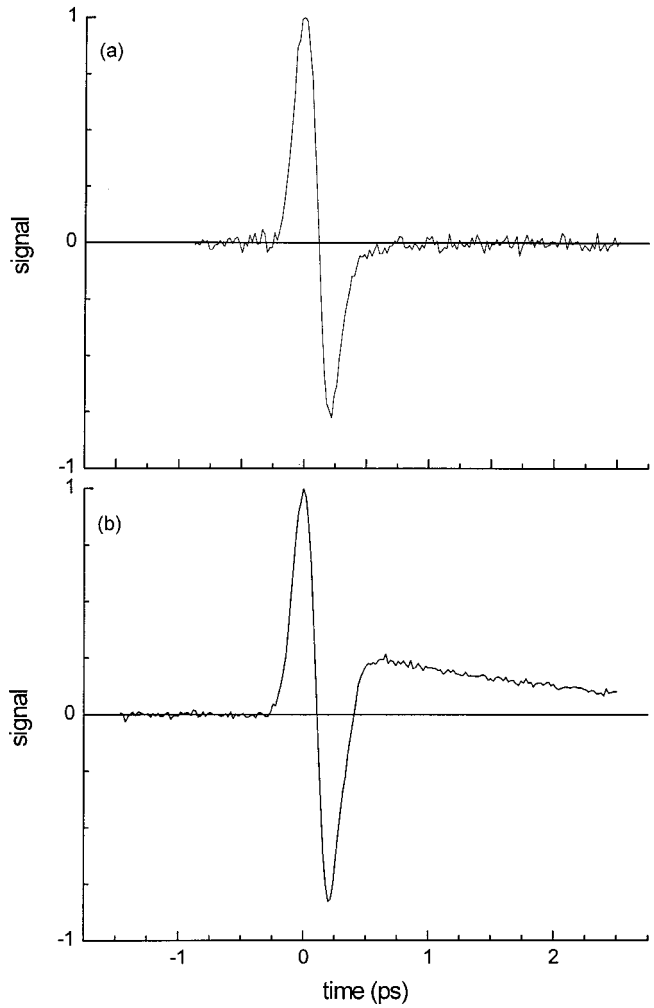

FIG. 2. Time-resolved IR pump-probe signals in (a) pure CCl_4 and (b) 2.5 mol % MeOD in CCl_4. As can be seen from the data, at early time the signals contain a nonresonant contribution arising from the CCl_4. In panel b, the beginning of the OD stretch vibrational pump-probe signal appears following the decay of the nonresonant solvent signal.

with increasing concentration agrees with reports for MeOH.[6,9,11–13,28] For 1 mol % samples, a sharp feature peaking at 2688 cm^{-1} dominates the spectrum. This feature is assigned to the nonhydrogen bond donating OD stretching mode. Frequently, this mode has been attributed to absorption by isolated, monomeric methanol molecules.[9] We follow the convention of Bakker and co-workers[17] labeling the OD of the monomeric MeOD α. With increasing concentration, this sharp feature persists and can be ascribed to true methanol monomers, α, and terminal, nonhydrogen bond donating OD moieties from methanol oligomers, designated β. The α and β moieties together give rise to the α/β absorption peak, the ''free OD peak.'' A broader feature appears to lower energy that has been attributed to the hydrogen-bonded methanol dimer or to an alcohol molecule that donates but does not accept a hydrogen bond, labeled γ.[6,13,28] An even broader feature at lower energy than the free OD stretching modes, α and β, and the γ band grows larger with increasing methanol concentration until it dominates the spectrum. In pure methanol, the free OD stretching mode is no longer observable. This spectral feature, referred to as the δ peak, has been attributed to methanol molecules in oligomers in which the OD is both a donor and an acceptor. In the lowest concentration (1%) spectrum in Fig. 1, the γ band is barely discernable. This feature is exaggerated by the fact that the extinction coefficients for the γ and δ bands are larger than the α/β extinction coefficients. The γ and δ extinction coefficients are factors of 3.5 and 10 greater than the α/β coefficients, respectively.[8] Therefore, the small amount of γ ODs present in the 1% sample is negligible.

Pump–probe data are shown in Figs. 2–6, as a function of delay between pump and probe pulses. In the highest concentration sample, the maximum bleaching of the absorption is ~0.5%. In the lowest concentration, the bleach is approximately a factor of 10 less. These data were collected with the polarizations of the pump and probe beams parallel to each other. Because the pump–probe signal is weak at low concentrations, 1 and 2.5 mol %, a signal from the CCl_4 (nonresonant electronic Kerr effect transient grating self-diffraction) contributes to the total signal at short time (see Fig. 2). The signal from pure CCl_4, shown in Fig. 2(a), decays to zero by 700 fs. While the signal from the 2.5 mol % sample, Fig. 2(b), displays the CCl_4 artifact, the additional contributions from the MeOD pump–probe signal can be clearly seen at times longer than ~700 fs. Figure 3 shows the decays for the 1 and 2.5 mol % samples beginning at 800 fs (after the CCl_4 nonresonant contribution to the signal has decayed to zero) along with a fit to a single exponential. The data fit to single exponentials very well. For both concentrations, the decay time is 2.15 ± 0.1 ps.

For the low-concentration samples, particularly the 1 mol % sample, the decay arises primarily from vibrational relaxation in monomers. The data indicate that the free OD stretching vibration is strongly coupled to other modes in the system, thereby causing it to lose its energy very rapidly. Vibrational relaxation can occur through a combination of

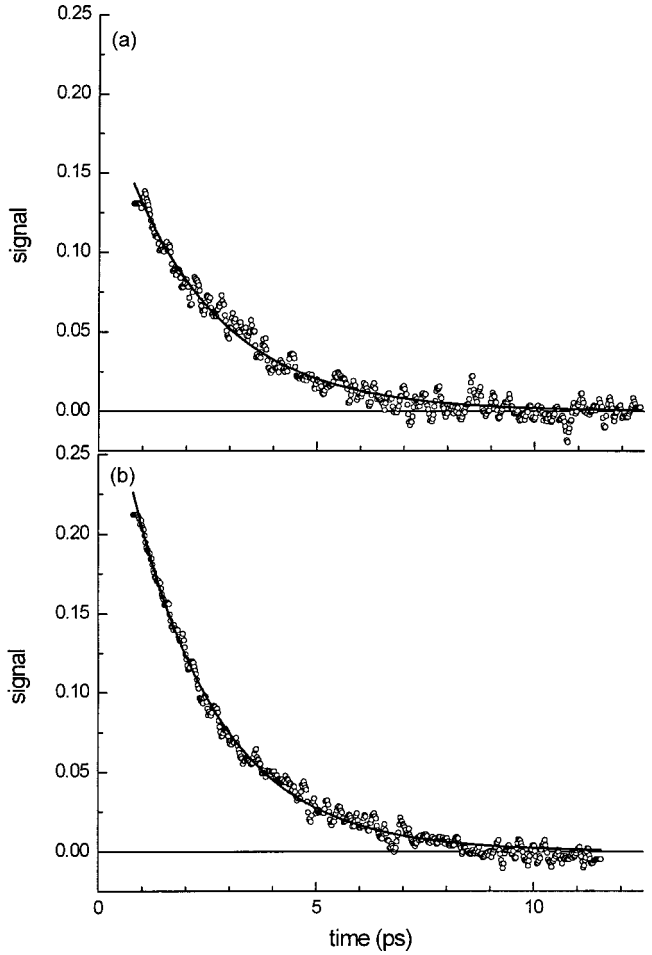

FIG. 3. Time-resolved IR pump-probe decays for (a) 1 and (b) 2.5 mol % MeOD in CCl_4 (open circles) with single exponential fits (solid lines) to the data. At both concentrations, the data fit well to a single exponential with the same decay time, 2.15 ± 0.1 ps.

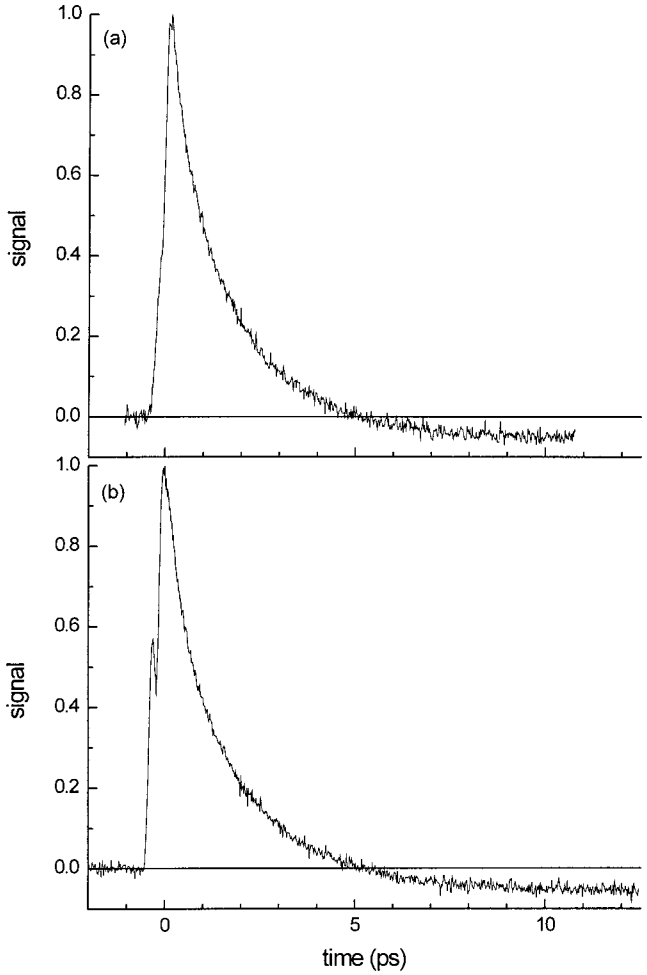

FIG. 4. Time-resolved IR pump-probe decays: short time decays (14.5 ps full scale) for (a) 3.75 and (b) 5 mol % MeOD in CCl_4. The signals decay below zero. The negative signal is caused by increased absorption over that which exists in the absence of IR excitation of the OD stretching vibration. The decay time is unchanged from the lower concentration data (Fig. 3). Hydrogen bond breaking produces additional free ODs, which absorb at the probe wavelength.

intramolecular and intermolecular pathways.[29] CCl_4 has low frequency internal modes and provides a continuum of bulk solvent modes that extend to ~ 150 cm^{-1}.[30] The likely path for vibrational relaxation of the OD stretch is to populate a number of other intramolecular MeOD modes and one or more modes of the continuum to satisfy energy conservation.

The time constant for vibrational relaxation that we measure, 2.15 ps, is significantly faster than that reported by Laenen and co-workers for low-concentration MeOH in CCl_4.[15,16] Our result is consistent with the estimation of the vibrational lifetime by Perelygin and Mikhailov.[18] It is possible that the difference lies in the deuteration of the MeOD molecule. The sum of the ν_6 methyl rock (1232 cm^{-1}) and the ν_5 valence angle deformation (1467/1447 cm^{-1}) could provide a resonant intramolecular pathway for the vibrational relaxation of the OD stretch.[31] Indeed, an *ab initio* calculation of the vibrational modes in methanol and its deuterated isotopomers showed significant Fermi interaction between the OD stretch and the $\nu_5 + \nu_6$ combination.[32] No Fermi interaction is observed for the other isotopomers of MeOH. The significantly higher energy of the OH mode makes the possibility of resonant energy transfer less likely for MeOH. Iwaki and Dlott[33] have shown that the OH mode in CH_3OH is not directly coupled to the CH stretching modes but can excite the methyl rock and deformation. They also found significant population of the C–O stretching mode.

At the higher concentrations (3.75 and 5 mol %) the pump–probe data display a bleach that rises within the laser-pulse width, followed by a decay to an amplitude below the baseline, as shown in Figs. 4 and 5. A signal that decays below zero is caused by increased absorption relative to the absorption that exists without IR excitation. Therefore, the data reveal that new absorbing species are being formed. Scans to longer times are shown in Fig. 5. By 10 ps, the data are clearly decaying back toward zero. However, for the length of the scan shown, the data do not return to zero. Even longer scans to 300 ps show a nondecaying small negative offset that does not return to the baseline. However, we can place an upper bound of 1 ms on the time scale for this recovery, as it is complete before the following laser pulse restarts the experiment. As discussed in the next section, the data were fit to a kinetic model. Within experimental and fitting uncertainty, the decay time for the initially positive

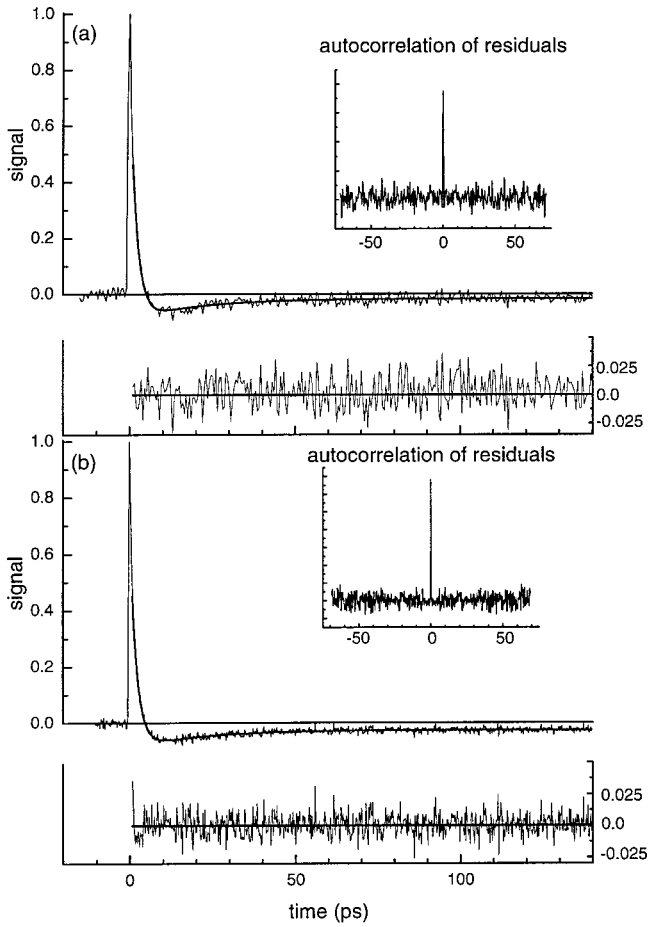

FIG. 5. Time-resolved IR pump-probe decays; long time decays (160 ps full scan) for (a) 3.75; and (b) 5 mol % and fits to the data using Eq. (9) (see text). The model that fits the data involves H-bond breaking and geminate (22 ± 1 ps) and nongeminate ($\gg300$ ps) recombination. Also shown are the residuals of the fit to Eq. (9) and the autocorrelations of the residuals, which demonstrate that the data do not deviate systematically from the fits.

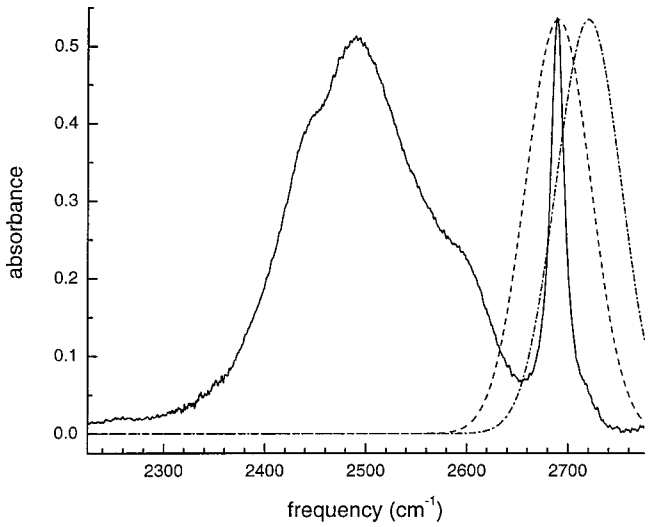

FIG. 6. Time-resolved IR pump–probe decays taken with the laser centered at 2690 cm^{-1} and 2720 cm^{-1}. The data are superimposable, demonstrating the complete lack of dependence on laser frequency. Therefore, the γ and δ portions of the MeOD spectrum do not contribute to the signal.

signal is the same as measured for the lower concentration samples, that is, 2.15 ps (Fig. 3). Two additional components, 22 ± 1 ps and >1 ns, comprise the recovery from the negative signal toward zero. Data were also collected with the probe polarization rotated to 54.7°, the magic angle. To within the S/N, the data with the probe polarization parallel to and at the magic angle with respect to the pump polarization are identical. We discuss the implications of the lack of an angular dependence below.

IV. KINETIC MODEL AND DISCUSSION

For the methanol molecules in solution that are true, isolated monomers, the vibrational relaxation is described by

$$\frac{dN^*_\alpha(t)}{dt} = -k_r N^*_\alpha(t), \tag{1}$$

where k_r is the rate for vibrational relaxation and $N^*_\alpha(t)$ is the number of vibrationally excited monomers (α's). Equation (1) has the solution

$$N^*_\alpha(t) = N^*_\alpha(0)e^{-k_r t}. \tag{2}$$

Because the data at low concentration also include a coherence artifact at early time [see Fig. 2(a)], the fits are started after the artifact has decayed to zero, that is at 800 fs after $t=0$. The data at low concentration (1 and 2.5 mol %) fit well to Eq. (2) ($1/k_r = 2.15\pm0.1$ ps). The spectral peak being excited and probed can have contributions from both α and β MeODs. Particularly in the 2.5 mol % sample, a significant portion of the signal arises from vibrational relaxation of β OD moieties. Therefore, within experimental uncertainty, the decays of the α and β species are the same.

At higher concentrations (3.75 and 5 mol %), the signal contains the decay of the initially excited vibrations, increased absorption, and the decay of the increased absorption on fast and slow time scales. Therefore, a more complicated kinetic model is necessary to describe the data. Consider the ensemble of β ODs (D not H-bonded) that are vibrationally excited. If the relaxation of the vibration leads to H-bond breaking in some fraction of the ensemble, then new absorbing species will be formed that contribute to absorption in the α/β peak. If the β OD is part of a dimer, there is initially one β OD and one γ OD. If the H-bond breaks, then both the β and γ ODs become α ODs. Where initially there was one absorber in the α/β peak, following H-bond breaking, there are now two absorbers. If the initially excited β OD is part of an oligomer, breaking the H-bond to the O of the β OD will produce an α and another β. If an H-bond is broken somewhere else in the oligomer, the initial β will remain a β and another β will be formed. In all cases, initially one absorber contributes to the α/β peak, but following the H-bond breaking, two absorbers contribute to the absorption. It is proposed that the increase in α/β peak absorption caused by H-bond breaking is responsible for the negative going signals shown in Figs. 4, 5, and 6. Reforming H-bonds will cause the extra absorption to decay away.

The number of vibrationally excited ODs is $N^*(t)$ with

$$N^*(t) = N^*_\alpha(t) + N^*_\beta(t), \tag{3}$$

TABLE I. Parameters derived from fits to Eq. (2) or (9) for MeOD in CCl_4.

Mol %	*1-F*	F_f	F_s	$1/k_r$ (ps)	$1/k_f$ (ps)	$1/k_s$ (ps)
1[a]	1	⋯	⋯	2.15±0.1	⋯	⋯
2.5[a]	1	⋯	⋯	2.15±0.1	⋯	⋯
3.75[b]	0.79±0.01	0.17±0.01	0.03±0.01	2.15[c,d]	22±1	≫300[d]
5[b]	0.79±0.03	0.15±0.02	0.05±0.01	2.15[c,d]	22±1	≫300[d]

[a]Fit to Eq. (2).
[b]Fit to Eq. (9).
[c]Determined from fits to low concentration data.
[d]Held constant during fitting.

where $N^*_\alpha(t)$ is the number of excited α's, and $N^*_\beta(t)$ is the number of excited β's at time t after the initial excitation. Of the initially excited ODs, some fraction (F) of them proceed to dissociate H-bonds, creating additional absorbers. Obviously, only excited β's break H-bonds; however, because we do not know the relative fraction of α and β free OD groups, we cannot determine the fraction of β's that break H-bonds, only the fraction of initially excited ODs (both α and β) that break H-bonds. $N^b_\beta(t)$ is the number of new absorbers formed by H-bond breaking. Of these, some reform H-bonds on a fast (f) time scale and some reform H-bonds slowly (s). Then,

$$N^b_\beta(t)=N^b_{\beta f}(t)+N^b_{\beta s}(t). \tag{4}$$

The fraction that reform rapidly is F_f, and the fraction that reform slowly is F_s

$$F=F_f+F_s. \tag{5}$$

In the experiments, the relaxation time (initial decay of the signal) does not change (within experimental error) when H-bond breaking is observed. For this reason we assume that following vibrational relaxation, for the fraction F of the molecules that are involved in H-bond breaking, the H-bond breaking is very fast compared to the vibrational relaxation rate. Therefore, for the subensemble of β's that leads to H-bonding breaking, the rate of H-bonding breaking is equal to k_r. (Another possibility will be discussed in the following.)

With these definitions and assumptions, a set of rate equations can be written to describe the kinetics of the system:

$$\frac{dN^b_{\beta f}(t)}{dt}=F_f k_r N^*(t)-k_f N^b_{\beta f}(t), \tag{6}$$

$$\frac{dN^b_{\beta s}(t)}{dt}=F_s k_r N^*(t)-k_s N^b_{\beta s}(t). \tag{7}$$

$N^*(t)$ is

$$N^*(t)=N^*(0)e^{-k_r t}, \tag{8}$$

because $N^*(t)=N^*_\alpha(t)+N^*_\beta(t)$, and the low-concentration samples show that $N^*_\alpha(t)$ and $N^*_\beta(t)$ have the same decay rate. The solutions of Eqs. (6) and (7) using Eq. (8) are combined to give the signal,

$$S(t)=2Q[N^*(0)e^{-k_r t}]+Q\left[\frac{k_r F_f N^*(0)}{k_r-k_f}(e^{-k_r t}-e^{-k_f t})+\frac{k_r F_s N^*(0)}{k_r-k_s}(e^{-k_r t}-e^{-k_s t})\right], \tag{9}$$

where Q is a constant that determines the absolute magnitude of the signal. It contains various experimental parameters such as the intensity of the pump pulse, the laser bandwidth, the extinction coefficient of the α/β peak, etc. The factor of two in front of the first term occurs because the initial decay of the signal is caused by both ground-state recovery and loss of stimulated emission from vibrationally excited molecules that have relaxed. The second and third terms in the second set of square brackets describe the signal that arises only from ground-state bleaching and recovery, that is, there is no stimulated emission contribution.

Equation (9) fits the data exceptionally well, as shown in Fig. 5. In addition to the fit that runs through the data points, the residuals and autocorrelation of the residuals are shown. The single spike centered at zero in the autocorrelation of the residuals demonstrates the high quality of the fit. Results from fits are given in Table I. The slow recovery appears to be a constant out to 300 ps. Therefore, k_s was fixed at 10^{-7} ps^{-1} (corresponding to a recombination time of ~10 μs). Fixing k_r at (1/2.15) ps^{-1} or letting it float as an adjustable parameter in the fits yields the same results. Therefore, k_r was held constant in the final fits to reduce the number of fitting parameters. That leaves only one adjustable rate constant, k_f. Because k_f is well-separated in time from the fast initial decay and the essentially time independent long time recovery, it can be obtained accurately; $1/k_f=22\pm1$ ps. The fractions F_f and F_s are also readily obtained because F_s is determined by the time independent offset at long time. The net result is that while there are quite a few parameters in Eq. (9), they are relatively independent and can be determined with considerable certainty. The results show that ~20% of the initially excited ODs result in H-bond breaking, that is, $F=0.2$. From the value of the long time offset, it is determined that $F_f=0.16$, and $F_s=0.04$.

At the higher concentrations (3.75 and 5 mol %), energy from a small fraction of the excited molecules breaks a hydrogen bond in a nearby OD group. The energy of the hydrogen bonds between MeOD molecules in bulk MeOD is on the order of 2000 cm^{-1},[34] and the laser frequency is 2690 cm^{-1}. Therefore, there is enough energy to break this bond.

Because the short time bleach decay occurs on the same time scale regardless of whether or not we observe hydrogen bond dissociation, these results suggest that the fast hydrogen bond dissociation is indirect. Vibrational energy relaxes from the initially excited β OD into a collection of internal modes of the same MeOD. Coupling of these excited vibrational modes to the H-bond breaks the H-bond. For example, the C–O stretch is certainly coupled to the H-bond through the oxygen. Other modes of the β MeOD can also be coupled to the H-bond. There will be a variety of different configurations for the γ and δ MeOD H-bonds to the oxygen of the β MeOD. It is possible that some subset of these configurations results in weaker H-bonds, H-bonds that are more strongly affected by the vibrations of the β MeOD excited by the relaxation of the OD stretch, or both (see the following).

We considered another possible mechanism to describe the data. This mechanism begins with excitation of β OD leading to H-bond breaking and depends on direct energy transfer from the initially excited β OD to a γ or δ OD that is H-bonded to the initially excited β MeOD. The γ and δ OD stretches are lower in energy than the β by $\sim$100 cm^{-1} and $\sim$200 cm^{-1}, respectively. A Förster-type hopping mechanism could transfer the energy downhill from the initially excited β OD to a γ or δ OD with the excess energy being absorbed by the solvent or low-frequency modes of the oligomer. Laenen and co-workers[35–40] hypothesized that energy transfer occurred prior to hydrogen bond dissociation following excitation of hydrogen bonded OH groups on methanol and ethanol. Once excited, a γ or δ H-bond could break by direct transfer of the OD stretching vibrational energy into the H-bond vibration. The direct breaking of H-bonds in this manner is the mechanism that has been invoked frequently to explain H-bond breaking following excitation of a H-bonded OH stretch.[17,35–38,41–43]

To test whether energy transfer from the initially excited β OD to a γ or a δ OD followed by H-bond breaking is responsible for the observed behavior, a different set of kinetic equations describing this alternative model was applied to the data. Because the energy would hop from the excited β OD to a γ or δ, in addition to k_r, another rate constant was included in the decay pathway for the initially excited β OD. At high MeOD concentration, for which most of the α/β peak is caused by β absorption, the additional energy-transfer pathway competes with vibrational relaxation. In this scenario, the $\sim$20% H-bond breaking that is observed for the high-concentration samples arises from the fraction of initially excited ODs that undergo energy hopping to a γ or δ OD. Unlike the first model presented, this alternative model fails to fit the data. To obtain sufficient H-bond breaking, the energy-transfer rate constant must be significant. This causes the decay of the initial signal to be too fast, well outside of experimental uncertainty.

As another test of the model, we also performed pump-probe experiments designed to ascertain whether signals from γ and δ moieties contribute to the signals measured at the α/β peak. Because the laser pulses are short (<200 fs), the laser spectrum is broad ($\sim$80 cm^{-1} FWHM) compared to the $\sim$20 cm^{-1} FWHM free OD peak of the steady-state IR spectrum. Figure 7 shows a representative spectrum, 2.5 mol %, of MeOD in CCl_4 along with the experimental pump–probe laser bandwidth at the two wavelengths used for time-resolved experiments. With the laser spectrum centered at the peak of the free OD feature, it overlaps the high-energy tail of the γ and δ band. Thus, the pump pulse could potentially excite hydrogen bond donating OD groups, γ's and δ's, leading to hydrogen bond breaking and an increase in the signal at the free OD frequency. By shifting the laser peak frequency $\sim$30 cm^{-1} to higher energy (2720 cm^{-1}), the pulse spectrum still overlaps the free OD peak well, but intersects the underlying γ and δ bands negligibly. A quantitative test was performed by calculating the overlap integral of the laser spectrum with the γ and δ bands of the MeOD spectrum. With the laser spectrum centered on the α/β peak, the overlap is very small. When the pulse is shifted to the blue, the overlap integral drops to essentially zero. Thus, any possible signal arising from oligomeric OD modes should be suppressed by shifting to higher energy. Decays measured at 2720 cm^{-1} cannot be distinguished from the decays measured at 2690 cm^{-1}, as shown in Fig. 6, demonstrating that γ and δ moieties do not contribute to the observed signals.

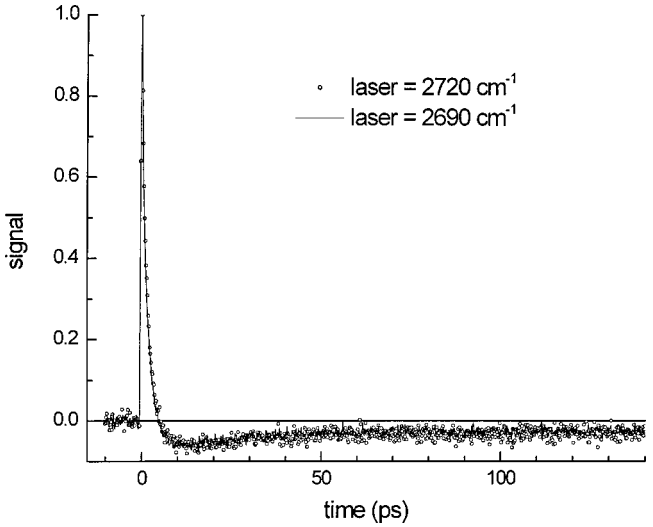

FIG. 7. Steady state spectrum of 2.5 mol % MeOD in CCl_4 (solid line) also showing the laser spectrum centered on the free OD spectral feature at 2690 cm^{-1} (dashed line) and shifted 30 cm^{-1} higher in energy to 2720 cm^{-1} (dotted–dashed line) to reduce overlap with the broad γ and δ MeOD features at lower energy. With the laser wavelength at 2720 cm^{-1}, there is essentially no overlap of the laser spectrum with the γ and δ portions of the MeOD spectrum.

The model that fits the data consists of vibrational relaxation of the β OD into internal modes of the same MeOD and possibly some solvent modes. Excitation of these modes causes H-bond breaking. The H-bond breaking does not occur by direct relaxation of an excited OD stretch into a highly excited H-bond mode that then breaks. In a mixed quantum-classical calculation of methanol dimer in CCl_4, Staib's[44] results indicate that energy deposited into a β OH can undergo vibrational relaxation and eventually lead to H-bond breaking. The results and model presented here contrast the results of Bakker and co-workers,[17,42,45] who reported a series of experiments in which energy deposited directly into hydrogen-bonded OH modes of water and alco-

hols led to rapid hydrogen bond dissociation. It was proposed that vibrational relaxation of the OH stretch directly excites the H-bond mode and breaks it. However, Bakker and co-workers' experiments were conducted on the broad oligomer peaks, not the isolated α/β peak studied here. Our results demonstrate that H-bond breaking can occur even when the initial excitation is of an OD stretch that is not H-bonded. The model that fits the data suggests that it is possible for the vibrational energy to relax into other intramolecular modes prior to hydrogen-bond dissociation.

The model discussed above states that β OD vibrational relaxation is followed by H-bond breaking. To explain why only a fraction of the initially excited β ODs result in H-bond breaking, we suggest that special structural configurations of H-bonded MeODs may be susceptible to H-bond breaking caused by interaction with a collection of excited vibrations. Previous experiments have reported that nearly all the molecules observed in 5 mol % samples are parts of oligomers,[10] indicating that β OD groups comprise nearly all of the free OD mode observed in 5 mol % samples. The negative signal (increased absorption) that we observe is not equal in amplitude to the initial ground-state bleach. Thus, only a fraction of the MeODs initially excited result in H-bond breaking, which points to the specialized nature of the H-bonds that do break. There is some experimental evidence to support this idea. In addition to measuring dynamics with the polarization of the probe beam parallel to the pump polarization, experiments were also conducted with the probe polarization at 54.7° (the magic angle). The decays showed no dependence on the relative polarizations of the pump and probe pulses. In fact, within the noise, the data collected for the two polarizations could be superimposed. This means that all of the free OD groups created by hydrogen-bond dissociation have their transition dipoles parallel, or close to parallel, to the transition dipoles of the originally excited OD groups. While configurations that allow adjacent methanol molecules to reside with their OD groups close to parallel to each other are somewhat unexpected, this may explain the relatively small fraction of hydrogen bonds broken compared to the total number of hydrogen bonds present.

The increased absorption signals that we observe at 3.75 and 5 mol % decay with two different time constants. The faster, 22 ps, decay agrees well with reports in the literature for geminate recombination.[17,35–39,41] The long time component may arise from nongeminate recombination due to solvent separation of MeOD molecules by CCl_4 molecules. MeOD can form weak H-bonds with CCl_4, ~10 times weaker than H-bonds between MeOD molecules.[46] Upon breaking the OD H-bond, direct interaction between the newly formed free OD and CCl_4 may inhibit rapid reformation of the original H-bond. Bakker and co-workers have recently observed a long time increased absorption signal when they performed ultrafast IR pump–probe experiments on the very broad oligomer band of pure alcohols and water.[42] In contrast to our interpretation, they attributed the long-lived transient increased absorption signal to local heating of the solution that led to blue-shifting of the oligomer absorption band. This explanation does not apply to the observations reported here for a number of reasons. First, careful power dependence studies revealed no changes in the decays or the long time recovery when the pump pulse energy was reduced. Second, the maximum pulse energies we used were more than an order of magnitude smaller than those used in related experiments.[4,17] Finally, and most convincingly, if the slow recovery portion of the data were due to local heating shifting the oligomer band toward the α/β peak, then we should have observed a smaller long term component of the increased absorption signal when we shifted the laser frequency 30 cm^{-1} higher in energy, because the oligomer peak is lower in energy than the α/β peak. As shown in Fig. 6, however, the scans with pump and probe radiation centered at 2690 and 2720 cm^{-1} can be superimposed.

V. CONCLUDING REMARKS

In summary, we have measured dynamics following excitation of the OD stretch in nonhydrogen bond donating OD groups of MeOD molecules in CCl_4 using ultrafast time-resolved transient infrared absorption spectroscopy. At low MeOD concentrations, the signals decay exponentially via vibrational relaxation with a 2.15 ps time constant. At higher MeOD concentrations, vibrational relaxation following excitation of the free OD mode leads to hydrogen bond dissociation. Reformation of the hydrogen bonds occurs on two distinct time scales, 22 ps and $\gg$300 ps.

An important result of this work is that it is possible for H-bonds to break following vibrational excitation of a non-H-bonded OD stretch. In previous studies, primarily of hydrogen bonded OH stretching modes of oligomers, H-bond breaking has been attributed to vibrational relaxation of the excited OH stretch directly into the OH···O hydrogen-bond stretch. The results presented here suggest that this need not always be the case. Further experiments are currently in progress on the oligomer bands of MeOD in CCl_4 and dilute MeOD in MeOH, as well as on the α/β peak of ethanol-*d* (EtOD) in CCl_4. These experiments will increase our understanding of H-bond dynamics and the potential differences between OD and OH hydrogen bonding.

ACKNOWLEDGMENTS

This work was supported by the National Institutes of Health (1RO1-GM61137), the National Science Foundation (DMR-0088942), and the Department of Energy (Grant No. DE-FG03-84ER13251). One of the authors (N.E.L.) gratefully acknowledges support for a sabbatical leave from the NSF POWRE program (CHE-0074913).

[1] F. Franks, *Mol. Recognit. Inclusion, Proc. Int. Symp. 9th*, 7 (1998).
[2] G. A. Jeffrey, J. Mol. Struct. **322**, 21 (1994).
[3] C. L. Perrin and J. B. Nielson, Annu. Rev. Phys. Chem. **48**, 511 (1997).
[4] J. C. Smith, D. Durand, M. Field, S. Furois-Corbin, G. R. Kneller, M. Nina, and B. Roux, NATO ASI Ser., Ser. C **435**, 489 (1994).
[5] *The Hydrogen Bond: Recent Developments in Theory and Experiments*, Vol. 1–3, edited by P. Schuster, G. Zundel, and C. Sandorfy (North-Holland, New York, 1976).
[6] O. Kristiansson, J. Mol. Struct. **477**, 105 (1999).
[7] J. E. Bertie, S. L. Zhang, H. H. Eysel, S. Baluja, and M. K. Ahmed, Appl. Spectrosc. **47**, 1100 (1993).

[8] J. E. Bertie and S. L. Zhang, Appl. Spectrosc. **48**, 176 (1994).
[9] O. D. Bonner, J. Chem. Thermodyn. **2**, 577 (1970).
[10] G. Kabisch and K. Pollmer, J. Mol. Struct. **81**, 35 (1982).
[11] M. C. R. Symons and V. K. Thomas, J. Chem. Soc., Faraday Trans. 1 **77**, 1883 (1981).
[12] H. C. Van Ness, J. Van Winkle, H. H. Richtol, and H. B. Hollinger, J. Phys. Chem. **71**, 1483 (1967).
[13] S. Singh, D. Schioeberg, and W. A. P. Luck, Spectrosc. Lett. **14**, 141 (1981).
[14] E. J. Heilweil, M. P. Casassa, R. R. Cavanagh, and J. C. Stephenson, J. Chem. Phys. **85**, 5004 (1986).
[15] R. Laenen and C. Rauscher, Chem. Phys. Lett. **274**, 63 (1997).
[16] R. Laenen and K. Simeonidis, Chem. Phys. Lett. **299**, 589 (1999).
[17] S. Woutersen, U. Emmerichs, and H. J. Bakker, J. Chem. Phys. **107**, 1483 (1997).
[18] I. S. Perelygin and G. P. Mikhailov, Chem. Phys. Reports **18**, 1023 (2000).
[19] J. R. Kuppers, J. Electrochem. Soc. **125**, 97 (1978).
[20] P. H. Davis, Ph.D., Stanford, 2001.
[21] M. M. Murnane, H. C. Kapteyn, C.-P. Huang, M. T. Asaki, and D. Garvey, in *Designs and Guidelines for Constructing a Mode-locked Ti:sapphire Laser, Rev. 1.6* (Washington State University, Pullman, WA, 1992).
[22] Y. Beaudoin, C. Y. Chien, J. S. Coe, J. L. Tapie, and G. Mourou, Opt. Lett. **17**, 865 (1992).
[23] B. E. Lemoff and C. P. J. Barty, Opt. Lett. **18**, 1651 (1993).
[24] O. E. Martinez, IEEE J. Quantum Electron. **23**, 59 (1987).
[25] M. Pessot, P. Maine, and G. Mourou, Opt. Commun. **62**, 419 (1987).
[26] T. R. Brewer, Ph.D., Stanford, 1996.
[27] S. Chen, Ph.D., Stanford, 1996.
[28] L. England-Kretzer, M. Fritzsche, and W. A. P. Luck, J. Mol. Struct. **175**, 277 (1988).
[29] V. M. Kenkre, A. Tokmakoff, and M. D. Fayer, J. Chem. Phys. **101**, 10618 (1994).
[30] P. Moore, A. Tokmakoff, T. Keyes, and M. D. Fayer, J. Chem. Phys. **103**, 3325 (1995).
[31] J. E. Bertie and S. L. Zhang, J. Mol. Struct. **413–414**, 333 (1997).
[32] A. Miani, V. Hanninen, M. Horn, and L. Halonen, Mol. Phys. **98**, 1737 (2000).
[33] L. K. Iwaki and D. D. Dlott, J. Phys. Chem. A **104**, 9101 (2000).
[34] H. Wolff, in *The Hydrogen Bond. Recent Developments in Theory and Experiments. III. Dynamics, Thermodynamics, and Special Systems*, edited by P. Schuster, G. Zundel, and C. Sandorfy (North Holland, Amsterdam, 1976), Vol. 3, p. 1227.
[35] R. Laenen, C. Rauscher, and A. Laubereau, J. Phys. Chem. A **101**, 3201 (1997).
[36] R. Laenen, C. Rauscher, and A. Laubereau, Chem. Phys. Lett. **283**, 7 (1998).
[37] R. Laenen, G. M. Gale, and N. Lascoux, J. Phys. Chem. A **103**, 10708 (1999).
[38] R. Laenen, C. Rauscher, and K. Simeonidis, J. Chem. Phys. **110**, 5814 (1999).
[39] N. Lascoux, G. M. Gale, and R. Laenen, J. Phys. IV **10**, r8/245 (2000).
[40] R. Laenen and K. Simeonidis, J. Mol. Struct. **552**, 147 (2000).
[41] S. Woutersen, U. Emmerichs, and H. J. Bakker, Laser Chem. **19**, 83 (1999).
[42] A. J. Lock, S. Woutersen, and H. J. Bakker, J. Phys. Chem. A **105**, 1238 (2001).
[43] R. Laenen and C. Rauscher, J. Chem. Phys. **107**, 9759 (1997).
[44] A. Staib, J. Chem. Phys. **108**, 4554 (1998).
[45] M. A. F. H. van den Broek, H. K. Nienhuys, and H. J. Bakker, J. Chem. Phys. **114**, 3182 (2001).
[46] M. A. Wendt, J. Meiler, F. Weinhold, and T. C. Farrar, Mol. Phys. **93**, 145 (1998).